

# Diffusive Motion in a 3-D Cluster in PK-4

Zian Wei, Bin Liu<sup>✉</sup>, John Goree, M. Y. Pustyl'nik, H. M. Thomas, V. E. Fortov, A. M. Lipaev, A. D. Usachev, V. I. Molotkov, O. F. Petrov, and M. H. Thoma

**Abstract**—Random motion of small solid particles is analyzed in a 3-D dusty plasma experiment under microgravity conditions. In this experiment, performed using the Plasmakristall-4 (PK-4) instrument on board the international space station, a cloud of microspheres was localized near a radio frequency coil that powered a neon plasma. We devised a method of correcting particle mean-square displacement (MSD) data to account for a small hydrodynamic flow. Using a time series of the MSD, we determined that random motion was nearly diffusive, with a diffusion coefficient of  $0.0017 \text{ mm}^2/\text{s}$ . Another measure of displacements, the probability distribution function, fits a Kappa distribution with  $\kappa = 6.9$ , indicating that the random motion was nearly Gaussian.

**Index Terms**—Diffusion, dusty plasma, microgravity, Plasmakristall-4 (PK-4).

## I. INTRODUCTION

THE random motion of small solid particles moving in a dusty plasma [1]–[3], which is a partially ionized gas containing highly charged micrometer-size solid particles, electrons, and ions can be observed experimentally [4]–[9]. The motion of the solid particles, which we also call dust particles, can be observed using video microscopy [10], [11]. Tracking the motion of dust particles from one video frame to the next allows measurements of random motion such as the mean-square displacement (MSD), the probability distribution function (PDF) of displacement, and the diffusion coefficient.

For 2-D dusty plasmas, both diffusive [5], [12]–[14] and superdiffusive [6]–[8], [15]–[17] motions have been reported. To distinguish these two kinds of motion, it is common to calculate [5] the MSD,  $\text{MSD} = \langle [x(t) - x(0)]^2 \rangle$ , from a particle's position  $x$ . By fitting to a power law

$$\text{MSD} \propto t^\alpha \quad (1)$$

one can characterize the random motion as diffusive if  $\alpha = 1$ , or superdiffusive if  $\alpha > 1$ . Superdiffusive motion can arise

Manuscript received September 24, 2018; revised December 11, 2018; accepted January 10, 2019. Date of publication January 31, 2019; date of current version July 9, 2019. This work was supported in part by DLR under Grant 50WM1441 and Grant 50WM1442 and in part by NASA-JPL through Iowa under Contract 1573629 and Contract 1579454. The review of this paper was arranged by Senior Editor T. Hyde. (Corresponding author: Bin Liu.)

Z. Wei, B. Liu, and J. Goree are with the Department of Physics and Astronomy, The University of Iowa, Iowa City, IA 52242 USA (e-mail: bin-liu@uiowa.edu).

M. Y. Pustyl'nik and H. M. Thomas are with Forschungsgruppe Komplexe Plasmen, Institut für Materialphysik im Weltraum, Deutsches Zentrum für Luft- und Raumfahrt, 82234 Wessling, Germany.

V. E. Fortov, A. M. Lipaev, A. D. Usachev, V. I. Molotkov, and O. F. Petrov are with the Joint Institute for High Temperatures, Russian Academy of Sciences, 125412 Moscow, Russia.

M. H. Thoma is with the I. Physikalisches Institut, Justus-Liebig-Universität Gießen, 35392 Giessen, Germany.

Color versions of one or more of the figures in this paper are available online at <http://ieeexplore.ieee.org>.

Digital Object Identifier 10.1109/TPS.2019.2893155

due to nonequilibrium effects, which are common in dusty plasmas that are both driven and dissipative [6], [17].

In addition to MSD, another measure of random displacements is the PDF. The PDF is a histogram of the displacement of particles over a specified time interval. In the limiting case, when the time interval is short compared to the collisional time scale, the PDF is the same as the velocity distribution function (VDF). For longer time intervals, the PDF is different from a VDF because the particle motion is not ballistic (i.e., inertial) but is deflected by collisions during the measurement interval. Experimenters have previously reported PDF measurements in laboratory dusty plasmas and the shape of these PDF curves is sometimes found to differ from a Gaussian distribution [6], [7], [16], [17]. A Gaussian distribution is expected in thermal equilibrium but laboratory dusty plasmas are not in equilibrium. While some experiments reported Gaussian distributions [18]–[22], a non-Gaussian distribution has also been reported for laboratory experiments with 2-D dust clouds [23], [24]. The phenomena of non-Gaussian statistics are sometimes linked to superdiffusion [6], [7], [16], [17].

Previous dusty plasma experiments for random motion [4]–[7], [25] were often 2-D, because of the effect of gravity. Under laboratory conditions, dust particles sediment to the bottom of a plasma, where there is a strong electric field that can levitate them. Under these conditions, the particle cloud has very few horizontal layers, and is often prepared with just a single horizontal layer, so that the experiments are said to be 2-D. To perform 3-D experiments requires overcoming the effects of gravity, which is best done using microgravity conditions, i.e., under free-fall conditions, as can be attained in parabolic aircraft flights and in spacecraft. Microgravity conditions allow forming larger 3-D dust clouds than is possible under 1-g conditions. They also offer the advantage of eliminating the need for large dc electric fields to provide levitation. The large electric fields can disturb the particles by causing a large ion flow. There have already been several reports of random motion in dusty plasmas under microgravity conditions [26], [27].

Here, we use flight data from the Plasmakristall-4 (PK-4) instrument, which is a dusty plasma instrument accommodated on the International Space Station (ISS) [28]. A noble-gas plasma is formed in a glass tube, and polymer microspheres are introduced to make a dusty plasma. The plasma can be powered by either a high-voltage dc power supply, a radio frequency (RF) power supply, or a combination of both. For imaging the dust particles, the instrument is equipped with high-resolution video cameras and a laser that illuminates a thin cross section within the dust cloud. It is possible to track the motion of individual dust particles in a PK-4 plasma. For the experiment reported in this paper,

the dust particles move slowly; their motion is mostly random, without any detectable waves. Consequently, the image data we analyze do not show any streaklike features, which can arise when particles move a significant distance during the exposure time for a video frame. Therefore, the data we analyze here allow identifying individual particles and tracking their motion from one frame to next.

In this paper, we report an experimental study of the random motion of dust particles in a PK-4 plasma. We will characterize the PDF and the MSD for random motion. The experimental run that we will analyze was performed under conditions, where the random motion is easily detected because it was not overwhelmed, as it is in some dusty plasma experiments, by waves or strong flows of dust particles.

## II. EXPERIMENT

For this paper, we carried out a survey of PK-4 flight experiments to identify an experimental run where random motion was the dominant motion for individual dust particles. In this survey, we excluded from consideration many experimental runs because they exhibited strong compressional wave motion, or organized hydrodynamic flows. As a result of this survey, we identified three experimental runs in Science Campaign 2, from the same day, June 16, 2016, which were all performed under similar conditions and with similar results. We will present here an analysis of one of these runs to characterize the random motion in a 3-D dusty plasma.

The data that we analyze were recorded for a plasma that was powered solely by applying RF induction. Before applying the RF power, the glass tube had been filled with neon to a pressure of 60 Pa, and then a plasma was ignited using only a dc power supply. Particles were injected, and the resulting particle cloud drifted toward the observation region, when the RF power was applied to a coil that was positioned near the middle of the glass tube. The RF power was 5 W in the forward direction, at 81.36 MHz. This method, which is the “combined transport and trapping technique” of [28], resulted in a cloud that remained in a stable location, which was desirable for our analysis of the random motion. In this experimental run, the hydrodynamic flow was small, with a speed of typically 0.08 mm/s.

The dust particles were melamine formaldehyde microspheres. They were injected by agitating shaker dispenser number 4, which was loaded with 1.3- $\mu\text{m}$ -diameter microspheres. The gas friction coefficient for this particle size [29], [30] was  $\nu_{\text{gas}} = 350 \text{ s}^{-1}$ . However, we note that we cannot exclude the possibility that larger particles were also present, for two reasons. First, 3.38- $\mu\text{m}$  particles used earlier in the campaign may have still been present in the chamber. Second, the particles might have sometimes been injected as doubles or triples rather than the desired single microspheres.

A cross section of the particle cloud was imaged by a particle-observation camera, which is the PO camera 2 of the PK-4 instrument [28]. A typical image is shown in Fig. 1. The camera was operated at a frame rate of 35.7 frames/s, corresponding to a time interval  $\Delta t = 0.028 \text{ s}$  between frames. We found that this frame rate is too slow to measure

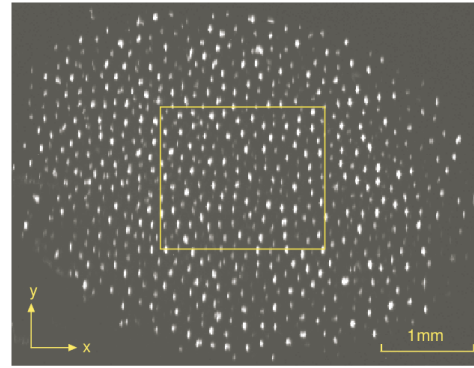


Fig. 1. Typical image of particle cloud. This still image is from one frame of a video recorded by a particle observation camera. The ROI where we analyze particle motion is indicated as a rectangle. Images were analyzed to measure the  $x$ ,  $y$  coordinates of particles and to track them from one video frame to the next.

a VDF for the small particles in this experiment but we can still measure a PDF for a time interval of  $\Delta t$ . The camera’s resolution was different by 0.5% in the horizontal and vertical directions [28]. We ignored this difference and used an averaged value of 0.0142 mm/pixel for the resolution, introducing random errors of less than 1% in our MSD curves. We analyzed a region of interest (ROI) of  $1.83 \times 1.53 \text{ mm}$ , as shown in Fig. 1. A cross section of the particle cloud was illuminated by a laser sheet, which the camera viewed at  $90^\circ$ . Due to the finite thickness of this laser sheet, about 110 particles are visible, within this ROI.

The general properties of the particle cloud, in the ROI, can be seen in Fig. 1. The arrangement of particles appears to be mainly isotropic; alignment of particles in strings, which is often seen in other dusty plasmas [31]–[33], is not prevalent in this experimental run in PK-4 with RF power. The 3-D pair correlation function,  $g(r)$ , as obtained from positions measured in still images [34], is shown in Fig. 2. From this pair correlation function, we obtained the 3-D particle number density  $n_{3\text{D}} = 380 \text{ mm}^{-3}$ , using the method of [34]. This measurement of 3-D number density will be used to obtain a dimensionless measure of the diffusion coefficient in Section IV-B. Combining this density and the 4.5 mm diameter of the cloud in Fig. 1, we can estimate the total number of particles in the 3-D cloud as  $\approx 18000$ .

## III. ANALYSIS METHODS

### A. Determination of Positions and Velocities

1) *Particle Tracking Velocimetry*: The position of an individual particle was measured using the moment method. Within a bit-map image corresponding to one video frame at time  $t$ , we identified particles within the ROI, and for each particle  $i$ , we measured its coordinates  $\mathbf{x}_i(t) = [x_i(t), y_i(t)]$  using the ImageJ image-analysis software [35]. We will later refer to these coordinates as our raw data for positions. To reduce measurement errors, we chose image-analysis parameters that were optimized as described in [10]. We repeated the measurement of particle coordinates for each of the 1000 video frames.

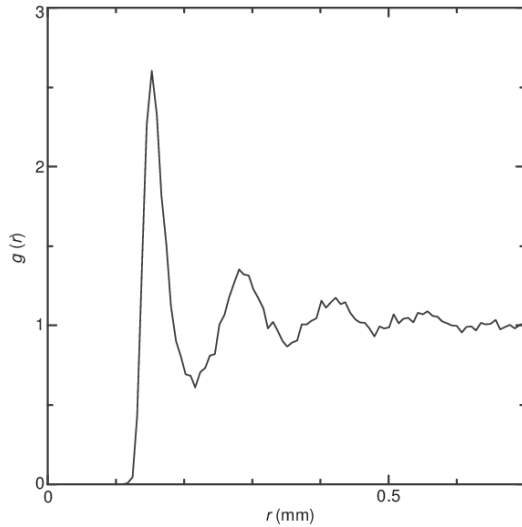


Fig. 2. 3-D pair correlation function  $g(r)$ , estimated from the 2-D  $g(r)$  using the method of [34]. We analyzed 1000 still images to prepare this graph. The shape of this function indicates a liquidlike microscopic structure. The location of the first peak allows a measurement of  $380 \text{ mm}^{-3}$  for the 3-D number density.

The particle-tracking velocimetry method [10], [11] was used to follow particles from one frame to the next. In this method, a particle is judged to be the same one, in two consecutive frames, if it moved by less than a search radius of 0.05 mm (3.66 pixels) of its previous position. We tracked each particle from one frame to the next, yielding a record of its coordinates in each frame. This record, which we call a “thread,” ultimately ends when a particle becomes indistinguishable from another, or when it vanishes from the ROI.

Particles often vanished because they moved perpendicular to the thin sheet of illuminating laser light, or less commonly by flowing out the ROI. The duration of long threads varied from particle to particle, and a distribution of their durations is shown in Fig. 3. From this distribution, we can characterize the half-life of threads as about five frames (0.14 s).

2) *Correcting for Flows:* Although we chose the data from an experimental run that had only a small hydrodynamic flow, it was still necessary for us to account for that flow in our analysis of the data. To do this, we devised a method of correcting particle displacements, for the small effects of the flow. Here, we describe the first part of this correction method to obtain a corrected particle displacement; in Section III-C, we will further present the method of correcting the MSD.

We devised a method to correct the displacement data to eliminate the small effect of the weak hydrodynamic flows to yield the fluctuating part of the particle position. This fluctuating part was calculated as

$$\tilde{\mathbf{x}}_i(t) = \mathbf{x}_i(t) - \mathbf{x}_{\text{flow}}(t) \quad (2)$$

where the last term is the hydrodynamic portion of the particle displacement

$$\mathbf{x}_{\text{flow}}(t) = \int_0^t \mathbf{v}_{\text{flow}}(t) dt \quad (3)$$

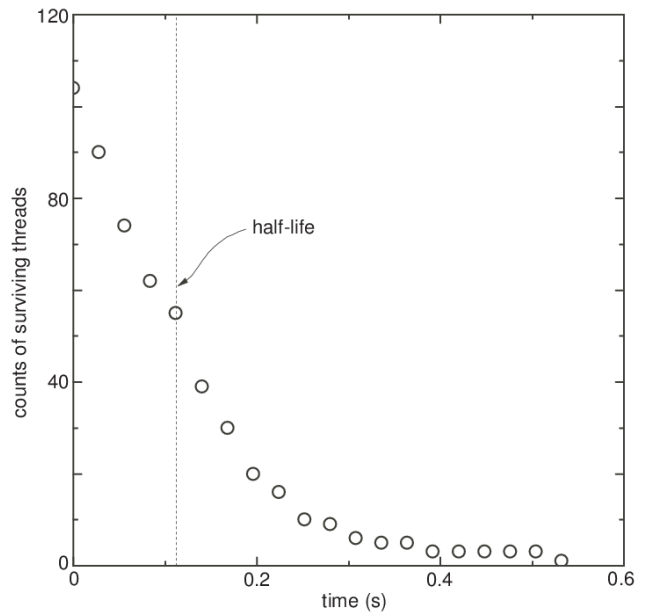


Fig. 3. Particle thread survival function. All the surviving threads, counted at a given time on the horizontal axis, originate at the same initial time zero (i.e., the same video frame). Due to motion having a component perpendicular to the thin illuminating laser sheet, a particle seen in one frame could be tracked only for a finite time. In other words, the “thread” of observations of a particle persists only a finite time. The half-life is the time when the count of surviving threads has diminished by one-half. Further analysis in this paper will be limited to a maximum time interval of two half-lives.

which can be calculated from our data for the hydrodynamic flow velocity  $\mathbf{v}_{\text{flow}}(t)$ . Since we chose to analyze the data where the flows were minimal, the last term in (2) was small, but we, nevertheless, correct for it.

Our data for the flow velocity  $\mathbf{v}_{\text{flow}}(t)$  were obtained in two straightforward steps. First, for each particle in the ROI, we calculated the difference in its position in two consecutive frames and then divided this difference by  $\Delta t$ , yielding a velocity for one particle at a given time  $t$ . Second, we averaged this velocity over all the observed particles in the ROI, yielding the hydrodynamic flow velocity  $\mathbf{v}_{\text{flow}}(t)$ .

### B. Determination of Probability Distribution Function

We prepared PDFs separately for displacements in the  $x$ -direction and  $y$ -direction. The PDF was prepared as the histogram of the displacement of individual particles for a specified time interval, which was an integer multiple of  $\Delta t$ . The input data for this histogram were the fluctuating part of the particle position  $\tilde{\mathbf{x}}_i(t)$  for each particle  $i$ .

To test whether the particle cloud obeys Gaussian statistics, we fit the PDF to both a Gaussian distribution

$$\propto \exp\left(-\frac{\Delta \tilde{\mathbf{x}}^2}{2\sigma^2}\right) \quad (4)$$

where  $\sigma$  characterizes the width of the Gaussian distribution and the Kappa distribution

$$\propto (1 + \beta \frac{\Delta \tilde{\mathbf{x}}^2}{\kappa})^{-\kappa} \quad (5)$$

where  $\beta^{-1}$  and  $\kappa$  characterize the width and the shape of the Kappa distribution, respectively. The Kappa distribution is a generalization of a Gaussian; its shape converges to a Gaussian shape in the limit  $\kappa \rightarrow \infty$ .

Some authors rewrite the Kappa distribution in an equivalent form, called a Tsallis distribution [6], [36], [37]. The Tsallis distribution has the same shape as a Kappa function, and it has a parameter,  $q = 1 + 1/\kappa$ . A Gaussian distribution is characterized by  $q = 1$ , while a non-Gaussian distribution with fat tails has  $q > 1$ . A larger value of  $q > 1$  indicates a more extreme deviation from Gaussian statistics. In Section IV-A, we will report both parameters,  $\kappa$  and  $q$ , to characterize our measured PDF.

### C. Determination of Mean-Square Displacement

We calculated the MSD as

$$\text{MSD} = \langle [\tilde{\mathbf{x}}_i(n\Delta t) - \tilde{\mathbf{x}}_i(0)]^2 \rangle. \quad (6)$$

The data for this calculation are the records of fluctuating particle position  $\tilde{\mathbf{x}}_i(t)$ . The unit of time is the interval between frames,  $\Delta t$ , and we record our results at times  $n\Delta t$ , where  $n$  is an integer. Here,  $\langle \cdot \rangle$  indicates a time average over all available data. To obtain the MSD, we first calculate a raw value

$$\text{MSD}_{\text{raw}} = \langle [\mathbf{x}_i(n\Delta t) - \mathbf{x}_i(0)]^2 \rangle \quad (7)$$

using the raw data  $\mathbf{x}_i(t)$  for particle positions. We then correct the MSD data for the effects of the small flow component. This correction consists of the last two terms of the following expression:

$$\text{MSD} = \text{MSD}_{\text{raw}} + \text{MSD}_{\text{flow}} + \text{MSD}_{\text{cross}} \quad (8)$$

where the term correcting for the flow is

$$\text{MSD}_{\text{flow}} = \langle [\mathbf{x}_{\text{flow}}(n\Delta t) - \mathbf{x}_{\text{flow}}(0)]^2 \rangle \quad (9)$$

and the crossterm for the correction is

$$\text{MSD}_{\text{cross}} = -2\langle [\mathbf{x}_{\text{flow}}(n\Delta t) - \mathbf{x}_{\text{flow}}(0)][\mathbf{x}_i(n\Delta t) - \mathbf{x}_i(0)] \rangle. \quad (10)$$

The final result of this correction is MSD, i.e., the left-hand side of (8). We then estimated the diffusion coefficient by using the Einstein relation [5]

$$\lim_{t \rightarrow \infty} \text{MSD} = 2Dt. \quad (11)$$

The diffusion coefficient  $D$  was obtained by fitting a graph of MSD curve versus time, at a large time.

## IV. RESULTS

### A. Probability Distribution Function

Our experimental result for the PDF is shown in Fig. 4. In preparing this graph, we calculated the PDF separately for motion in the  $x$ -direction and  $y$ -direction. As mentioned above, a PDF is prepared for a specified time interval, which for Fig. 4 was a relatively small value  $\Delta t = 0.028$  s.

A small deviation from a Gaussian shape can be seen in the PDF (see Fig. 4). A Gaussian distribution, (4), fits the

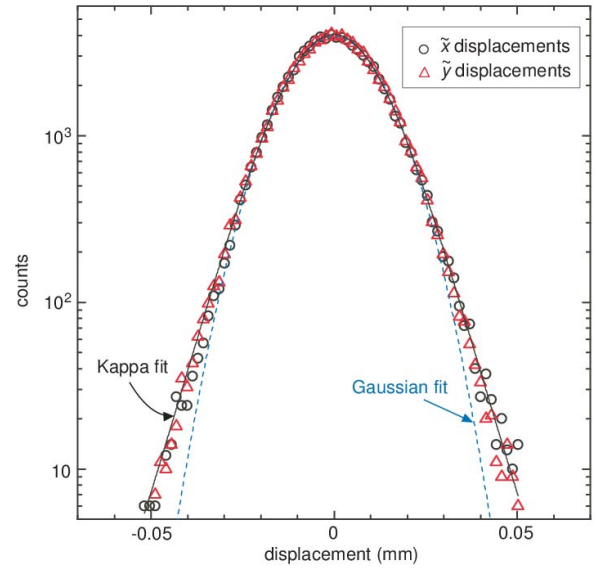


Fig. 4. PDFs for displacements calculated separately in  $x$ -direction and  $y$ -direction, prepared as histograms of the displacement during a measurement time interval  $\Delta t = 0.028$ s. These two PDF curves were averaged (not shown here), and then fit to (4) and (5), yielding a Gaussian distribution and a Kappa distribution, respectively. The data are fit better by a Kappa distribution, with  $\kappa = 6.9$ , than by a Gaussian, due to a fat tail.

observed PDF data only for the core of the distribution at small displacements. The width coefficient  $\sigma$  in (4) was found as a free parameter in the fit to have the value  $\sigma = 0.012$  mm. For displacements larger than 0.03 mm during this time interval, the distribution's tail is fatter than for a Gaussian.

We find that a Kappa distribution fits the PDF better than a Gaussian, as shown in Fig. 4. We obtained a good fit to (5), yielding the fit parameters,  $\kappa = 6.9$  and  $\beta = 4160$ . The equivalent parameter for a Tsallis distribution is  $q = 1.15$ . While this value of  $q$  is certainly larger than unity, it is not so much larger as to say that the distribution is strongly non-Gaussian; instead, we could say that the distribution is nearly Gaussian. Since the PDF is nearly Gaussian, it is meaningful to discuss the random motion in terms of a diffusion coefficient, as we will do below.

Based on our measurement of the parameter  $\kappa$ , we can describe our system as resembling that near equilibrium. As prescribed in [38] and [39], the value of  $\kappa$  can indicate how far a system is from thermal equilibrium. Two regions can be distinguished: near equilibrium for  $\kappa > 2.5$  and far equilibrium for  $1.5 < \kappa < 2.5$ . Our measured value,  $\kappa = 6.9$ , is well within the near-equilibrium region, indicating that our system resembles systems near thermal equilibrium.

As a further characterization of the nonequilibrium conditions, we can estimate the fraction of nonthermal (non-Maxwellian) particle density as compared to the total particle density. Using [40, eq. (3)], we estimated that the fraction of non-Maxwellian particles is about 12%, for our measured value  $\kappa = 6.9$ . This small fraction of non-Maxwellian particles carry about 30% of the total particle energy, as estimated using [41, Fig. 8(e)]. It is this small fraction of particles that are responsible for the formation of the Kappa distribution in our experimental system.

It is worthwhile to mention that this result, for a nearly Gaussian PDF, is slightly different from that of a previous microgravity dusty plasma experiment [27], from an earlier experiment in PK-4 using different experimental conditions (larger particles and a slightly different gas pressure). In that earlier experiment, the VDF (i.e., VDF, which is the PDF in the limit of small time interval  $\Delta t$ ) was found to have the shape of a Maxwellian “core” plus a Kappa-distribution function “halo.” The halo, which describes the energetic tail of the distribution in that experiment, was characterized by  $\kappa = 1.72$ , which is equivalent to  $q = 1.58$ . For the experiment studied in this paper, we did not measure the VDF because the smaller particle size made it impractical to measure instantaneous velocity, at the frame rate that was used, and for this reason, we cannot make a direct comparison to the earlier results of [27]. We can mention that for the present experiment, the PDF is fit well by a Kappa distribution by itself; the fit does not require the sum of a Maxwellian plus a Kappa distribution.

The observation of a Kappa distribution is generally interpreted as an indication of some nonequilibrium effects that are not fully overcome by stochastic collisions with a thermal bath [42]. In our experimental system, nonequilibrium effects are expected because a gas-discharge plasma is typically a driven-dissipative system [6], [17]. Here, we can mention several sources that could cause nonequilibrium effects in our experiment. Most significantly, energetic flowing ions can impart significant energy to dust particles. In our microgravity experiment, particles reside mainly in the bulk plasma, where we expect the ion flow effects to be less severe than in the sheath region of a plasma where dust particles reside in ground-based experiments. Nevertheless, flowing ions are still present, as seen from the presence of dust acoustic waves in some other experiments performed in PK-4 [43]. In addition, from a perspective of the dynamics of dust particles, strongly correlated particle motion like turbulent flows could also cause the system to deviate from Gaussian statistics [44], although we do not expect this effect to be strong because the particle flow velocity was small and we did not detect strong turbulent behavior. In general, the magnitude and character of nonequilibrium effects can vary from one experiment to another depending on the plasma conditions, so that the signature of nonequilibrium effects, as seen in a distribution function, will not always be the same, even when comparing two experiments performed in the same plasma device.

The dusty plasma literature is generally lacking theories that would allow a quantitative prediction of the value of  $\kappa$ . As discussed earlier, we generally expect that nonequilibrium conditions, such as ion flows, turbulence, and waves, will be responsible for the formation of the Kappa distribution. However, we are unable to quantify their specific effects on the formation of the Kappa distribution in our experiment, due to a lack of theoretical foundation.

We note that there are existing theories [45]–[50] regarding the formation of the Kappa distribution in some solar and space plasmas. For example, in a theoretical model for solar flares [48], it has been demonstrated that a Kappa distribution can be a solution of the Fokker–Planck equation that considers turbulence as a stochastic acceleration mechanism and

Coulomb collisions as a frictional mechanism. The value of  $\kappa$  is predicted as the ratio of a collision term divided by a turbulence term. However, this model is intended for weakly coupled plasma, where the stochastic acceleration and the Coulomb collisions assumed are likely to differ from those in strongly coupled dusty plasma. Due to these differences, the theoretical approach in [48] may not have the specific capability of predicting  $\kappa$  for dusty plasma, although we can suggest that such an approach could be extended to ion-flow-driven dusty plasma in the future. Doing so would require not only that the Fokker–Planck equation is applicable to the strongly coupled motion of dust particles but also that a stochastic acceleration mechanism due to ion-flow-driven instabilities could be modeled. If these two requirements can be met, one could follow a prescription like that in [48], possibly predicting a Kappa-like distribution and the value of Kappa. However, such a theoretical effort is beyond the scope of this paper.

### B. Mean-Square Displacement

Our result for the MSD is shown in Fig. 5. In the top, which is for the displacements in the  $x$ -direction, we show a curve for MSD, which is our main result. Also shown are curves for  $\text{MSD}_{\text{raw}}$ , and the correction terms  $\text{MSD}_{\text{flow}}$  and  $\text{MSD}_{\text{cross}}$ . These four quantities are defined in (6), (7), (9), and (10) and are related by (8), to yield MSD. The data shown are for values of time ranging from one to ten video frames. In the bottom, for displacements in the  $y$ -direction, the two correction terms are too small to appear in the graph, so that the raw and corrected MSD values are nearly the same.

The MSD data are found to fall nearly on a straight line of unity slope on the log–log plot, indicating that motion is nearly diffusive. This result can be seen in Fig. 5 by comparing the corrected MSD data points to the dashed reference line, which has a slope of unity. To support this conclusion, we fit the MSD data to a power law, (1). This fit yields the MSD exponent  $\alpha = 0.99$  and  $0.91$  for motion in the  $x$ -direction and  $y$ -direction, respectively.

Our MSD data in Fig. 5 do not indicate a transition from ballistic to the diffusive motion. Such a transition is a feature often seen in self-diffusion, separating ballistic motion at small times (with an MSD exponent of 2), and diffusive motion at long times (with an exponent of 1). This transition between ballistic and diffusive motion is generally expected to occur on a time scale where the effects of collisions begin to accumulate, in the motion of individual particles that are undergoing self-diffusion. Previous experiments [6] and simulations [16] of dusty plasmas, for a 2-D particle layer in the presence of gas at a low pressure, have indicated a transition at a time  $\approx 5 \omega_{\text{pd}}^{-1}$ , where  $\omega_{\text{pd}}$  is the dusty plasma frequency. The present experiment was different because it was performed in a 3-D dust cloud, and with higher gas pressure and smaller dust particles. As a background medium, gas causes frictional drag, which could be a complicating factor in the transition from ballistic to the diffusive motion. Our lack of an observation of the transition might be due to either the high level of neutral gas friction or a high thermal velocity.

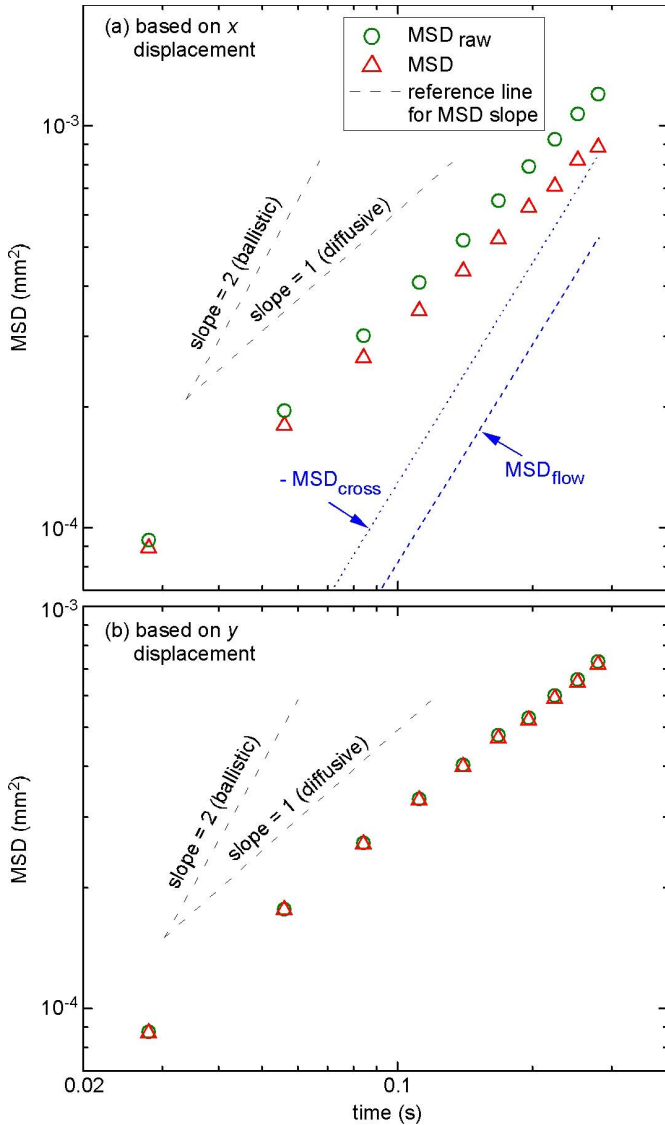


Fig. 5. MSD. (a) Four measures of a particle's displacement in the  $x$ -direction (top). The corrected and raw values, MSD and MSD<sub>raw</sub>, are shown as triangles and circles, respectively. The corrected value was obtained by adding the correction terms MSD<sub>flow</sub> (dashed line) and MSD<sub>cross</sub> (dotted line). (b) Corresponding results for displacements in the  $y$ -direction; however, the two correction terms are too small to appear in the graph, so that the raw and corrected MSD values are nearly the same (bottom).

Having shown that the random motion is nearly diffusive, as indicated by the slope of the MSD data, we can now obtain a diffusion coefficient. We fitted the MSD using the Einstein relation [i.e., (11)] and we did this separately for motion in the  $x$ -direction and  $y$ -direction. Averaging these two results for the MSD data, we find  $D = 0.0017 \text{ mm}^2/\text{s}$ . In dimensionless units, we can write this result as  $Dn_{3D}^{2/3}v_{\text{gas}}^{-1} = 2.5 \times 10^{-4}$ .

As a confirmation, we also estimated the diffusion coefficient using another method. Integrating the velocity autocorrelation function, the Green–Kubo relation [51], yields an estimate of  $D = 0.0015 \text{ mm}^2/\text{s}$ . This value is close to that of our MSD result. Of these two values, we consider the MSD result to be more reliable, because the data for the velocity

autocorrelation function had few data points in its main peak, due to the slow camera frame rate.

For comparison, we note that our measured diffusion coefficient,  $D = 0.0017 \text{ mm}^2/\text{s}$ , is smaller than that in a previous microgravity experiment performed using a parabolic aircraft flight [52]. In that previous experiment, the diffusion coefficient was found to be in the range of  $0.35\text{--}6.4 \text{ mm}^2/\text{s}$ , which was several orders of magnitude higher than our result. A different diffusion coefficient in these two experiments could be due to several factors. First, the diffusion in the previous parabolic flight experiment was driven by a concentration gradient during the process of phase separation, while the diffusion in our experiment was primarily due to thermal fluctuations. Second, the gas frictional forces in the two experiments were different, because of different particle sizes and gas pressure. Third, the plasma in the previous parabolic flight experiment was generated using a capacitively coupled RF discharge between two parallel plate electrodes, while in our PK-4 experiment, the RF power was inductively coupled to the plasma using an RF coil.

## V. CONCLUSION

The random motion of dust particles was analyzed for a 3-D cloud of dust particles in a plasma under microgravity conditions. The PDF was found to be nearly Gaussian. We found a good fit to a Kappa distribution with a relatively high value of  $\kappa = 6.9$ .

The MSD was found to obey a power law with an exponent of nearly unity, over all time scales that we measured. This result indicates that the random motion is nearly diffusive, in contrast to previous ground-based experiments where the motion was slightly superdiffusive with an exponent of about 1.1 [6].

The diffusion coefficient for this dusty plasma, with its 3-D cloud of small-diameter dust particles under microgravity conditions, was found to be  $D = 0.0017 \text{ mm}^2/\text{s}$ .

To obtain this diffusion coefficient, we analyzed data for conditions where hydrodynamic flows were very weak, and we corrected for those weak flows using a method presented here.

## ACKNOWLEDGEMENT

The authors would like to thank the joint ESA/Roscosmos “Experiment Plasmakristall-4” onboard the International Space Station.

## REFERENCES

- [1] J. H. Chu and I. Lin, “Direct observation of Coulomb crystals and liquids in strongly coupled RF dusty plasmas,” *Phys. Rev. Lett.*, vol. 72, no. 25, pp. 4009–4012, Jun. 1994.
- [2] H. Thomas, G. E. Morfill, V. Demmel, J. Goree, B. Feuerbacher, and D. Möhlmann, “Plasma crystal: Coulomb crystallization in a dusty plasma,” *Phys. Rev. Lett.*, vol. 73, no. 5, pp. 652–655, Aug. 1994.
- [3] A. Melzer, T. Trottenberg, and A. Piel, “Experimental determination of the charge on dust particles forming Coulomb lattices,” *Phys. Lett. A*, vol. 191, pp. 301–308, Aug. 1994.
- [4] W.-T. Juan and L. I., “Anomalous diffusion in strongly coupled quasi-2D dusty plasmas,” *Phys. Rev. Lett.*, vol. 80, no. 14, pp. 3073–3076, Apr. 1998.

- [5] S. Nunomura, D. Samsonov, S. Zhdanov, and G. Morfill, "Self-diffusion in a liquid complex plasma," *Phys. Rev. Lett.*, vol. 96, no. 1, Jan. 2006, Art. no. 015003.
- [6] B. Liu and J. Goree, "Superdiffusion and non-Gaussian statistics in a driven-dissipative 2D dusty plasma," *Phys. Rev. Lett.*, vol. 100, no. 5, Feb. 2008, Art. no. 055003.
- [7] S. Ratynskaia *et al.*, "Superdiffusion and viscoelastic vortex flows in a two-dimensional complex plasma," *Phys. Rev. Lett.*, vol. 96, no. 10, Mar. 2006, Art. no. 105010.
- [8] T. Ott, M. Bonitz, Z. Donkó, and P. Hartmann, "Superdiffusion in quasi-two-dimensional Yukawa liquids," *Phys. Rev. E, Stat. Phys. Plasmas Fluids Relat. Interdiscip. Top.*, vol. 78, no. 2, Aug. 2008, Art. no. 026409.
- [9] S. A. Khrapak, O. S. Vaulina, and G. E. Morfill, "Self-diffusion in strongly coupled Yukawa systems (complex plasmas)," *Phys. Plasmas*, vol. 19, no. 3, Mar. 2012, Art. no. 034503.
- [10] Y. Feng, J. Goree, and B. Liu, "Accurate particle position measurement from images," *Rev. Sci. Instrum.*, vol. 78, no. 5, May 2007, Art. no. 053704.
- [11] Y. Feng, J. Goree, and B. Liu, "Errors in particle tracking velocimetry with high-speed cameras," *Rev. Sci. Instrum.*, vol. 82, no. 5, May 2011, Art. no. 053707.
- [12] O. S. Vaulina and S. V. Vladimirov, "Diffusion and dynamics of macro-particles in a complex plasma," *Phys. Plasmas*, vol. 9, no. 3, pp. 835–840, Mar. 2002.
- [13] H. Ohta and S. Hamaguchi, "Molecular dynamics evaluation of self-diffusion in Yukawa systems," *Phys. Plasmas*, vol. 7, no. 11, pp. 4506–4514, Oct. 2000.
- [14] T. S. Strickler, T. K. Langin, P. McQuillen, J. Daligault, and T. C. Killian, "Experimental measurement of self-diffusion in a strongly coupled plasma," *Phys. Rev. X*, vol. 6, no. 2, May 2016, Art. no. 021021.
- [15] B. Liu, J. Goree, and O. S. Vaulina, "Test of the Stokes-Einstein relation in a two-dimensional Yukawa liquid," *Phys. Rev. Lett.*, vol. 96, no. 1, Jan. 2006, Art. no. 015005.
- [16] B. Liu and J. Goree, "Superdiffusion in two-dimensional Yukawa liquids," *Phys. Rev. E, Stat. Phys. Plasmas Fluids Relat. Interdiscip. Top.*, vol. 75, no. 1, Jan. 2007, Art. no. 016405.
- [17] B. Liu, J. Goree, and Y. Feng, "Non-Gaussian statistics and superdiffusion in a driven-dissipative dusty plasma," *Phys. Rev. E, Stat. Phys. Plasmas Fluids Relat. Interdiscip. Top.*, vol. 78, no. 4, Oct. 2008, Art. no. 046403.
- [18] V. Nosenko, J. Goree, and A. Piel, "Laser method of heating monolayer dusty plasmas," *Phys. Plasmas*, vol. 13, no. 3, Mar. 2006, Art. no. 032106.
- [19] J. Kong, K. Qiao, L. S. Matthews, and T. W. Hyde, "Temperature measurement of a dust particle in a RF plasma GEC reference cell," *J. Plasma Phys.*, vol. 82, Sep. 2016, Art. no. 905820505.
- [20] J. D. Williams, "Application of particle image velocimetry to dusty plasma systems," *J. Plasma Phys.*, vol. 82, Jun. 2016, Art. no. 615820302.
- [21] R. Fisher and E. Thomas, "Observation and model of an ellipsoidally symmetric velocity space distribution in a weakly-coupled dusty plasma," *Phys. Plasmas*, vol. 18, Nov. 2011, Art. no. 113701.
- [22] V. Nosenko, S. Zhdanov, A. V. Ivlev, G. Morfill, J. Goree, and A. Piel, "Heat transport in a two-dimensional complex (dusty) plasma at melting conditions," *Phys. Rev. Lett.*, vol. 100, Jan. 2008, Art. no. 025003.
- [23] A. K. Mukhopadhyay and J. Goree, "Two-particle distribution and correlation function for a 1D dusty plasma experiment," *Phys. Rev. Lett.*, vol. 109, no. 16, Oct. 2012, Art. no. 165003.
- [24] Z. Haralson and J. Goree, "Temperature dependence of viscosity in a two-dimensional dusty plasma without the effects of shear thinning," *Phys. Plasmas*, vol. 23, no. 9, Sep. 2016, Art. no. 093703.
- [25] V. E. Fortov, O. F. Petrov, O. S. Vaulina, and K. G. Koss, "Brownian motion of dust particles in a weakly ionized plasma," *JETP Lett.*, vol. 97, no. 6, pp. 322–326, May 2013.
- [26] V. E. Fortov *et al.*, "Transport of microparticles in weakly ionized gas-discharge plasmas under microgravity conditions," *Phys. Rev. Lett.*, vol. 90, no. 24, Jun. 2003, Art. no. 245005.
- [27] B. Liu *et al.*, "Particle velocity distribution in a three-dimensional dusty plasma under microgravity conditions," *AIP Conf. Proc.*, vol. 1925, Jan. 2018, Art. no. 020005.
- [28] M. Y. Pustynnik *et al.*, "Plasmakristall-4: New complex (dusty) plasma laboratory on board the International Space Station," *Rev. Sci. Instrum.*, vol. 87, no. 9, Sep. 2016, Art. no. 093505.
- [29] B. Liu, J. Goree, V. Nosenko, and L. Boufendi, "Radiation pressure and gas drag forces on a melamine-formaldehyde microsphere in a dusty plasma," *Phys. Plasmas*, vol. 10, no. 1, pp. 9–20, Jan. 2003.
- [30] B. Liu *et al.*, "Experimental observation of cnoidal waveform of nonlinear dust acoustic waves," *Phys. Plasmas*, vol. 25, no. 11, p. 113701, 2018.
- [31] A. V. Ivlev *et al.*, "First observation of electrorheological plasmas," *Phys. Rev. Lett.*, vol. 100, no. 9, Mar. 2008, Art. no. 095003.
- [32] M. A. Fink, M. H. Thoma, and G. E. Morfill, "PK-4 science activities in micro-gravity," *Microgr. Sci. Technol.*, vol. 23, no. 2, pp. 169–171, Feb. 2011.
- [33] O. Arp, J. Goree, and A. Piel, "Particle chains in a dilute dusty plasma with subsonic ion flow," *Phys. Rev. E, Stat. Phys. Plasmas Fluids Relat. Interdiscip. Top.*, vol. 85, no. 4, Apr. 2012, Art. no. 046409.
- [34] B. Liu, J. Goree, and W. D. S. Ruhunusiri, "Characterization of three-dimensional structure using images," *Rev. Sci. Instrum.*, vol. 86, no. 3, Mar. 2015, Art. no. 033703.
- [35] C. A. Schneider, W. S. Rasband, and K. W. Eliceiri, "NIH Image to ImageJ: 25 years of image analysis," *Nature Methods*, vol. 9, no. 7, pp. 671–675, Jun. 2012.
- [36] C. Tsallis, "Possible generalization of Boltzmann-Gibbs statistics," *J. Stat. Phys.*, vol. 52, nos. 1–2, pp. 479–487, Jul. 1988.
- [37] C. Tsallis and D. J. Bukman, "Anomalous diffusion in the presence of external forces: Exact time-dependent solutions and their thermostatical basis," *Phys. Rev. E, Stat. Phys. Plasmas Fluids Relat. Interdiscip. Top.*, vol. 54, no. 3, pp. R2197–R2200, Sep. 1996.
- [38] G. Livadiotis and D. J. McComas, "Invariant Kappa distribution in space plasmas out of equilibrium," *Astrophys. J.*, vol. 741, no. 2, Oct. 2011, Art. no. 88.
- [39] G. Livadiotis and D. J. McComas, "Exploring transitions of space plasmas out of equilibrium," *Astrophys. J.*, vol. 714, no. 1, pp. 971–987, Apr. 2010.
- [40] M. Oka, S. Ishikawa, P. Saint-Hilaire, S. Krucker, and R. P. Lin, "Kappa distribution model for hard X-ray coronal sources of solar flares," *Astrophys. J.*, vol. 764, no. 1, Jan. 2013, Art. no. 6.
- [41] M. Oka, S. Krucker, H. S. Hudson, and P. Saint-Hilaire, "Electron energy partition in the above-the-looptop solar hard X-ray sources," *Astrophys. J.*, vol. 799, no. 2, Jan. 2015, Art. no. 129.
- [42] V. Pierrard and N. Meyer-Vernet, "Electron distributions in space plasmas," in *Kappa Distributions: Theory and Applications in Plasmas*, G. Livadiotis, Ed. 1st ed. Cambridge, MA, USA: Elsevier, 2017, ch. 11, pp. 465–479.
- [43] S. Jaiswal *et al.*, "Dust density waves in a dc flowing complex plasma with discharge polarity reversal," *Phys. Plasmas*, vol. 25, no. 8, Aug. 2018, Art. no. 083705.
- [44] P. H. Yoon and G. Livadiotis, "Nonlinear wave-particle interaction and electron kappa distribution," in *Kappa Distributions: Theory and Applications in Plasmas*, G. Livadiotis, Ed., 1st ed. Cambridge, MA, USA: Elsevier, 2017, ch. 8, pp. 363–398.
- [45] M. Oka *et al.*, "Electron power-Law spectra in solar and space plasmas," *Space Sci. Rev.*, vol. 214, no. 5, Aug. 2018, Art. no. 82.
- [46] B. D. Shizgal, "Kappa and other nonequilibrium distributions from the Fokker-Planck equation and the relationship to Tsallis entropy," *Phys. Rev. E, Stat. Phys. Plasmas Fluids Relat. Interdiscip. Top.*, vol. 97, no. 5, May 2018, Art. no. 052144.
- [47] M. Lazar, H. Fichtner, and P. H. Yoon, "On the interpretation and applicability of  $k$ -distributions," *Astron. Astrophys.*, vol. 589, May 2016, Art. no. A39.
- [48] N. H. Bian, A. G. Emslie, D. J. Stackhouse, and E. P. Kontar, "The formation of Kappa-distribution accelerated electron populations in solar flares," *Astrophys. J.*, vol. 796, no. 2, Nov. 2014, Art. no. 142.
- [49] C.-Y. Ma and D. Summers, "Correction to 'formation of power-law energy spectra in space plasmas by stochastic acceleration due to whistler-mode waves,'" *Geophys. Res. Lett.*, vol. 26, no. 8, pp. 1121–1124, Apr. 1999.
- [50] A. Hasegawa, K. Mima, and M. Duong-Van, "Plasma distribution function in a superthermal radiation field," *Phys. Rev. Lett.*, vol. 54, no. 24, pp. 2608–2610, Jun. 1985.
- [51] J.-P. Hansen and I. R. McDonald, *Theory of Simple Liquids*, 4th ed. Oxford, U.K.: Elsevier, 2013.
- [52] C. Killer, T. Bockwoldt, S. Schütt, M. Himpel, A. Melzer, and A. Piel, "Phase separation of binary charged particle systems with small size disparities using a dusty plasma," *Phys. Rev. Lett.*, vol. 116, no. 11, Mar. 2016, Art. no. 115002.

Authors' photographs and biographies not available at the time of publication.